Green Chemistry

PAPER

View Article Online
View Journal | View Issue

Cite this: *Green Chem.*, 2015, **17**, 2418

Sonochemical synthesis of HSiW/graphene catalysts for enhanced biomass hydrolysis†

Miri Klein,[a] Alexander Varvak,[b] Elad Segal,[a] Boris Markovsky,[a] Indra Neel Pulidindi,[a] Nina Perkas[a] and Aharon Gedanken*[a,c]

Received 24th December 2014,
Accepted 16th January 2015

DOI: 10.1039/c4gc02519a

www.rsc.org/greenchem

Hydrolysis of biomass for the production of glucose was studied. Silicotungstic acid (HSiW) was deposited on graphene by an ultrasound-assisted procedure. The catalyst (HSiW/G) was characterized using a variety of physico-chemical methods. Homogeneous distribution of HSiW on the surface of graphene was demonstrated. The hydrolysis of glycogen was performed with a HSiW/G catalyst by hydrothermal treatment. The yield of glucose (66 wt%) obtained was about 8 times higher than that obtained with the same amount of bare HSiW. Stability of the HSiW/graphene even after 3 repeated uses was confirmed. The mechanism of the enhancement of catalytic activity was discussed in terms of a special interaction between the graphene support and HSiW and also the appearance of hydrophobic cavities on the surface of graphene. The formation of these cavities facilitates the anchoring of glycogen to the catalyst surface and promotes the attack of protons that leads to selective, rapid, and efficient hydrolysis.

Introduction

Current energy systems are based mainly on fossil resources such as coal, petroleum and natural gas. However, the rapid consumption of natural resources has prompted researchers on finding renewable energy sources to meet increasing demand.[1]

Biomass is a sustainable source of organic carbon, which is considered as part of the solution to producing biofuels and chemicals.[2,3] Biomass is obtainable world-wide in the form of organic materials such as grass, wood, agricultural crops and glycogen.[4] Biomass hydrolysis by enzymes is a common method for biofuel production, but it has low efficiency and high cost.[5] Many studies have been done on the hydrolysis of biomass to glucose with mineral acids,[1,4,6] but the large scale use of acids causes several problems such as reactor corrosion, further degradation of monomers, recovery of catalysts, and requires special treatment of the acid residue producing much waste.[7]

Solid acid catalysts have various advantages over liquid acid catalysts, such as: simple product separation, possible recycling, and less damage to the reactor.[1] Heteropoly acids (HPAs) are a type of solid acid consisting of transition metal–oxygen anion clusters. HPAs have received much attention due to their fascinating architectures and excellent physicochemical properties, such as Brønsted acidity, high proton mobility and good stability. They dissolve in polar solvents and release H^+, whose acidic strength is stronger than typical mineral acids like sulfuric acid.[8,9]

Lately, HPAs have been widely used as homogeneous catalysts for biomass conversion. Shimizu *et al.* reported HPAs ($H_3PW_{12}O_{40}$, $H_4SiW_{12}O_{40}$) and salts of metal cations (Mn^+) and $PW_{12}O_{40}^{3-}$ ($M_{3/n}PW_{12}O_{40}$) for selective hydrolysis of cellobiose and cellulose to glucose in an aqueous phase.[10] In that study the glucose yield after 24 h was in the following order: $H_3PW_{12}O_{40}$ (53 wt%) > $H_4SiW_{12}O_{40}$ (51 wt%) > $HClO_4$ (42 wt%) > H_2SO_4 (29 wt%) > H_3PO_4 (12 wt%). This indicates that a stronger Brønsted acid is more favourable for the hydrolysis of a glycosidic bond.[10] Juan *et al.* investigated the potential of $H_3PW_{12}O_{40}$ for the hydrolysis of cellulose to glucose under hydrothermal conditions. A remarkably high yield of glucose (50.5%) and selectivity higher than 90% at 453 K were found after 2 h.[11] Ogasawara *et al.* showed that a highly negatively charged polyanion ($H_5BW_{12}O_{40}$) promoted efficient conversion of crystalline cellulose into water-soluble saccharides in concentrated aqueous solutions (82% total yield and 77% glucose yield, based on reacting cellulose with a 0.7 M $H_5BW_{12}O_{40}$ solution).[12] The heteropoly acids could be separated from the

[a]*Department of Chemistry and the Center for Advanced Materials and Nanotechnology, Bar Ilan University, Ramat Gan, 52900 Israel. E-mail: gedanken@mail.biu.ac.il*
[b]*The Mina and Everard Goodman Faculty of Life Sciences, Bar Ilan University, Ramat Gan, 52900 Israel*
[c]*Department of Materials Science & Engineering, National Cheng Kung University, Tainan 70101, Taiwan*

† Electronic supplementary information (ESI) available: S1. XRD diffraction of graphene commercial and HSiW/G catalyst; S2. Typical HPLC chromatogram of the hydrolyzate. See DOI: 10.1039/c4gc02519a

homogeneous solution and recycled by extraction with diethyl ether,[11] but this process takes a long time, and the extraction is not complete. Some traces of the catalyst remain in the product.

Graphene has received much attention from researchers in the past few years due to its exceptional electronic, mechanical, and optical properties, high surface area, and biocompatibility. It is used in various applications including electrochemical, biosensors,[13] transistors for nano-electronics,[14] solar cells[15] *etc*. Because of its excellent adsorptive ability, graphene is also used as a support for heterogeneous catalysts. J. M. Yang *et al.* loaded platinum nanoparticles on sulfonated graphene and used it as a conductive polymer for fuel-cell applications.[16] S. M. Choi *et al.* synthesized surface-functionalized graphene nanosheets (GNS) with 80 wt% Pt loading with a particle size of less than 3 nm. These Pt/GNS catalysts provided improved mass specific activity in alcohol electro-oxidation.[17] Polyoxometalate–graphene composites were recently exploited for supercapacitor and electrocatalytic (nitrite electro-oxidation) applications.[18,19]

Graphene supported catalysts have also demonstrated high activity in biomass conversion.[1,20] Supported solid acid catalysts on graphene oxide and on sulfonated graphene oxide nanosheets have been prepared by Wei *et al.*[21] The experimental results indicated that the catalytic activity of the synthesized catalyst was superior to that of other solid acid catalysts and also better than that of H_2SO_4. They assigned the high activity of the catalyst to the formation of hydrophobic cavities on the graphene sheet containing oxygen groups on its surface. Kitano *et al.* reported on the enhancement of the hydrolysis of β-1,4-glucan on graphene-based amorphous carbon bearing SO_3H, COOH, and OH groups. Their results suggested that the synergistic combination of high densities of the functional groups bonded to amorphous carbon causes the efficient hydrolysis of β-1,4-glucan including cellulose.[22]

Glycogen, a water soluble polysaccharide of glucose (Scheme 1), is a better feedstock for glucose production than lignocellulosic biomass as it needs no additional pre-treatment. The synthesis of glycogen from CO_2 by photosynthesis and its subsequent hydrolysis to glucose with high selectivity make glycogen an abundant and renewable feedstock for the production of glucose.[23] Even though animal remains are the only source of glycogen as of now, currently immense research is underway to produce glycogen from cyanobacteria whereas CO_2 is used as feedstock for glycogen synthesis.[24] Owing to such possibilities, strategies need to be developed for the effective conversion of glycogen to glucose, which was the objective of this study.

The hydrolysis of glycogen to glucose is a critical step in the production of bioethanol and other value added chemicals. In the previous work Gedanken *et al.* converted glycogen to glucose with HCl and HPAs as a catalyst. The glucose yields obtained with HCl and HSiW catalysts were 62 and 63 wt%, respectively.[4] However, the process was corrosive and the product separation after the hydrolysis was time consuming and involved organic solvents.[4] We believe that the development of a new supported catalyst can overcome these disadvantages.

In this article we report on a new silicotungstic acid (HSiW) catalyst supported on graphene (HSiW/G). The catalyst preparation was performed by a sonochemical method which has been proven to be an effective technique for the synthesis of supported catalysts.[25,26] The catalytic activity of HSiW/G was studied for the hydrolysis of glycogen. This supported catalyst could be easily separated from the reaction mixture. The physical and chemical properties of the catalysts were studied by the following methods: X-ray diffraction (XRD), transmission electron microscopy (TEM), high resolution scanning electron microscopy (HR-SEM), N_2 isothermal adsorption–desorption (Brunauer–Emmett–Teller, BET), FT-IR and Raman spectroscopy, inductively coupled plasma (ICP) analysis, and dynamic light scattering (DLS).

Results and discussion

Catalyst characterization

The morphology of the catalyst HSiW/G was studied by using HR-SEM (Fig. 1).

Sheets with layered structures were observed in the case of commercial graphene (Fig. 1a). The HSiW/G catalyst showed randomly oriented spherical particles of HSiW, in the range of 100–250 nm, on the graphene sheets (Fig. 1b). It could be seen that the original smooth surface of graphene was partly changed after deposition of HSiW, but the layered structure of graphene was not destroyed. The amount of HSiW on graphene was found to be 2.5 wt% by ICP analysis.

The influence of sonication on the morphology and size of HSiW was studied by TEM and DLS analysis. The TEM image

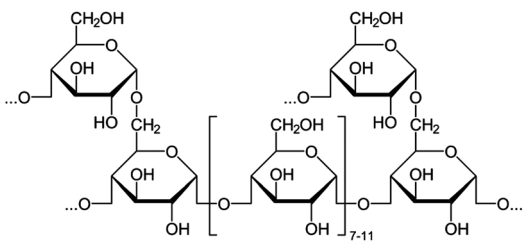

Scheme 1 Chemical structure of glycogen, a rich and abundant source of glucose.

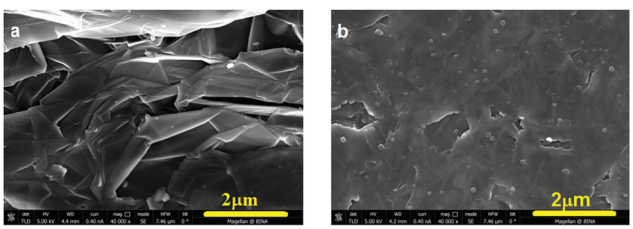

Fig. 1 HR-SEM images of (a) commercial graphene and (b) graphene coated with HSiW using the sonochemical method.

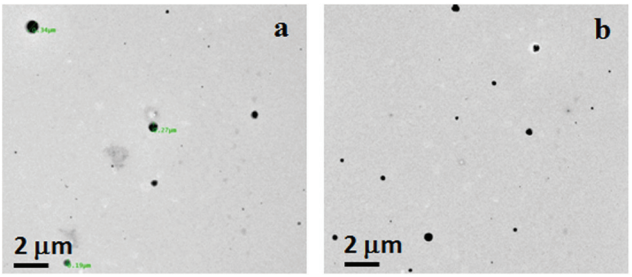

Fig. 2 TEM images of the HSiW after (a) 1 h stirring and (b) 1 h sonication.

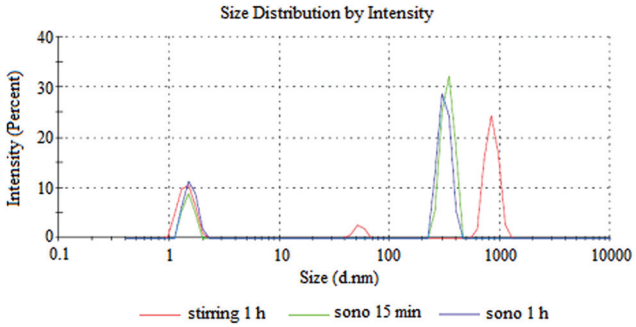

Fig. 3 DLS plot depicting the size distribution of HSiW particles after 15 min sonication, 1 h sonication and 1 h stirring.

indicated that after 1 h of sonication of HSiW in ethanol without graphene, spherical HSiW nanoparticles were formed with sizes in the range of 100–400 nm (Fig. 2(b)). After the same period (1 h) of regular stirring of HSiW in ethanol the spherical particles of a slightly larger size in the range of 200–500 nm were found (Fig. 2(a)). In addition to the large particles, very small particles were also observed in both treatments. The TEM results confirmed that the spherical nanoparticles on the surface of graphene shown in Fig. 1 were indeed HSiW.

In addition to TEM, DLS analysis was also employed to measure the particle size of HSiW upon different treatments (Fig. 3). The results were in agreement with the TEM images. It was found that with an increase in the sonication time from 15 to 60 min the average particle size decreased from 380 to 340 nm. Jafari *et al.* made similar observations in the reduction of particle size of colloidal nanosilica from 170 to 60 nm as the sonication time is increased from 0.25 to 60 min.[27] Such a reduction of particle size results in an improved catalytic performance of HSiW/G in the hydrolysis process.

The XRD patterns of the commercial graphene and HSiW/G catalyst are shown in Fig. S1.† A sharp diffraction peak at 2θ = 28° indicating an interlayer distance of 0.335 nm is typical of graphene. The XRD results of HSiW/G are similar to those of graphene, which indicates that the HSiW adsorption process does not change the lattice constants of graphene.

The amount of HSiW on graphene (2.5 wt%) was analyzed by ICP. This loading of HSiW on the catalyst is too low to be

Table 1 BET measurements

Sample	Surface area [m^2 g^{-1}]	Average pore radius [Å]	Pore volume [mL g^{-1}]
Graphene	73	29	0.11
HSiW/G	52	26	0.07
HSiW	1.8	10	0.009

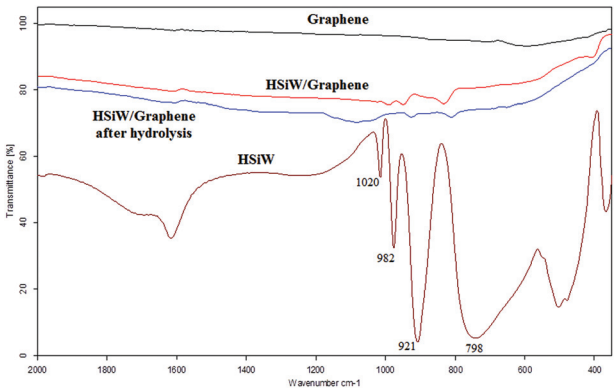

Fig. 4 FT-IR spectra of graphene, HSiW/G and HSiW.

detected by XRD. Even with the higher loadings of HSiW (10 wt%) in the HSiW/G, the XRD pattern did not change. This could be due to the amorphous nature of HSiW on graphene.

The textural properties of HSiW/G catalysts were studied by BET analysis (Table 1).

The BET specific surface area for HSiW supported on graphene with 2.5% loading reached 52 m^2 g^{-1}. The data in Table 1 show that the specific surface area of the HSiW/G catalysts is reduced by 30% as compared to the commercial graphene. The surface area of pure solid HSiW is only 1.8 m^2 g^{-1}. Thus, the deposition of HSiW on graphene with HSiW led to a better dispersion of active components onto the graphene surface. The pore size and pore volume of the HSiW/G are slightly small compared to the commercial graphene. This could be because of partial blocking of the small graphene pores (diameter ≈ 1.2 nm)[28] with the HSiW Keggin (≈1.5 nm) units.

The FT-IR spectra of the bare graphene, HSiW and HSiW/G catalyst are shown in Fig. 4. As shown before by P. S. Wate *et al.*,[29] the FT-IR spectra of graphene did not show any significant absorption peaks over the range of 400–2000 cm^{-1}.

The FT-IR spectrum of HSiW demonstrated four characteristic peaks at 1020, 982, 921, and 798 cm^{-1} that are assigned to the stretching modes of Si–O, W═O, W–Oe–W, and W–Oc–W, respectively.[30]

In the spectrum of HSiW/G the peaks in the region of 1020–780 cm^{-1} are very weak and slightly shifted to lower wavelengths. This shift indicates a strong interaction between graphene and the catalyst, causing the weakening of the various bonds. A similar effect was observed by Chen *et al.*[30] upon stabilization of HSiW by organic molecules. The FT-IR results clearly demonstrated the fact that HSiW was effectively

deposited on graphene and its strong interaction with the support.

The Raman spectra of the bare graphene, HSiW and HSiW/G catalyst are shown in Fig. 5.

The most prominent features in the Raman spectra of graphene are the G-band appearing at 1587 cm^{-1} and the D-band appearing at 1353 cm^{-1} (Fig. 5a). The G-band represents the planar configuration sp^2 bonded carbon that constitutes the graphene lattice. It is associated with the doubly degenerate (iTO and LO) phonon mode (E_{2g} symmetry). The D-band corresponds to the disordered sample or to the edge of a graphene.[31,32]

The Raman spectroscopy technique was used extensively for observing the Keggin structure and also for proving its presence on the graphene.[28,33,34] The Raman spectrum of commercial HSiW (Fig. 5b) showed the most intense bands at 1000 cm^{-1}, 974 cm^{-1}, 551 cm^{-1} and 224 cm^{-1} assigned to stretching of W═O, bending of W–Oc–W, O–Si–O, and WO_3 vibrations, respectively. These signals are typical of Keggin structure.[28] In order to study the possible interaction between HSiW and the graphene support we focused on the Raman spectral domain of HSiW (Fig. 5b).

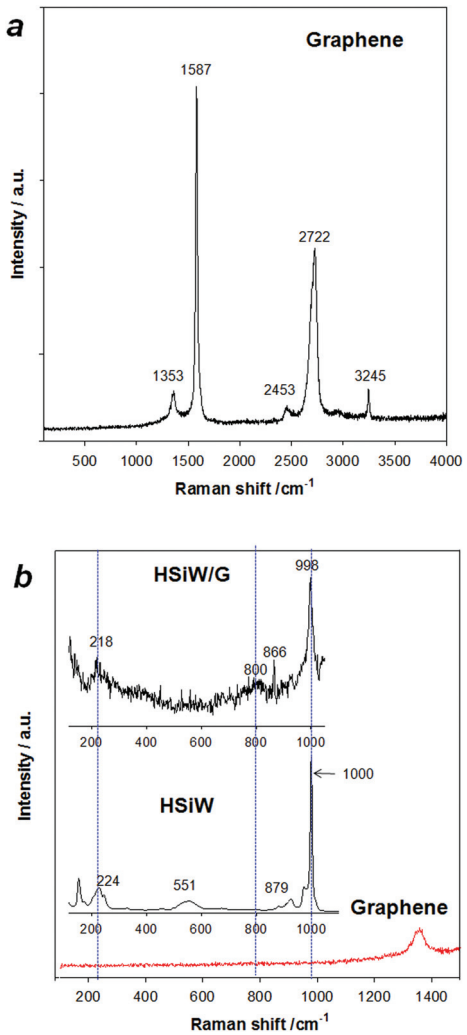

Fig. 5 Raman spectrum of graphene in full range (a), and Raman spectra of graphene, HSiW and HSiW/G (b). Dashed blue lines are eye-guides.

The Raman spectrum of HSiW/G is similar to that of the bare heteropoly acid. The spectrum showed peaks at 998 cm^{-1}, 866 cm^{-1} and 218 cm^{-1} for the W═O stretching, W–Oc–W bending mode, and WO_3 bending, indicating the preservation of the Keggin structure of the HSiW on the surface of graphene. However, a shift in two bending modes is noticed. The W–O–W and WO_3 modes decreased from 879 to 866 cm^{-1} and from 224 to 218 cm^{-1}, respectively. Such a shift might be due to the strong interaction of HSiW with the graphene support, which correlates with the FT-IR result. A similar shift to lower wave-numbers was also observed in the Raman spectra of HSiW deposited on Al_2O_3 and SiO_2.[28,33,34]

XRD, Raman and HR-SEM studies indicated that the graphene layers are not damaged during sonochemical synthesis of the HSiW/G catalyst. Based on the Raman results it could also be argued that the units of the HSiW were not destroyed during the deposition and they are well dispersed on the surface of graphene. The HSiW is homogeneously distributed on the surface of graphene and strongly anchored to the support. Even after the catalytic hydrolysis of glycogen, the bands corresponding to HSiW were observed in the FT-IR spectra (Fig. 4).

The sonochemical deposition of HSiW on the graphene substrate is presented in Scheme 2.

Our explanation of the ultrasound assisted coating is based on the phenomena of cavitation, formation, growth and implosive collapse of the acoustic bubbles in the liquids. The nanoparticles (NPs) of HSiW created in the liquid under ultrasound waves are thrown to the solid by microjets and shock waves, which are the after effects of the cavitation collapse.[35,36] The speed and power of the microjets are extremely high (>500 m s^{-1}), causing the strong anchoring of the NPs to the surface of the substrate. Low frequency ultrasound has diverse applications. Fang *et al.* utilized ultrasound for promoting a variety of crucial reactions (dewaxing, removal of impurities, particle size reduction, isolation of chemicals from biomass, delignification, fractionation, reduction of crystallinity and acceleration of saccharification and fermentation) involved in the conversion of biomass to biofuels.[37] Shewale *et al.* utilized the potential of 20 kHz ultrasound for the particle size reduction of sorghum slurry from 302 to 115 μm (38%) which resulted in improved glucose yield. The particle size reduction was due to the disruption of the protein matrix and the amylose–lipid

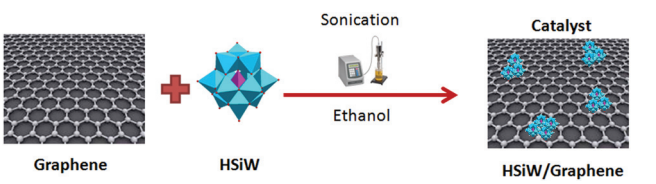

Scheme 2 Synthesis of the HSiW/G catalyst by the sonochemical method.

complexes surrounding the starch granules.[38] Such physical effects that are due to acoustic cavitation were well documented.[39]

Glycogen hydrolysis under hydrothermal reaction conditions

The glycogen hydrolysis was carried out under hydrothermal conditions in an autoclave. ^{13}C NMR spectra of the products obtained with three types of catalysts (bare HSiW, bare graphene and HSiW/G) are shown in Fig. 6.

As suspected, no glycogen conversion was observed when only graphene was used as the catalyst (Fig. 6a). With HSiW, complete conversion of glycogen to glucose (60.3 (C6), 69.2 (C4), 72.4 (C2), 73.7 (C3), 75.3 (C5), 92 (C 1α) and 95.3 (C 1β)) was obtained (Fig. 6c). With the HSiW/G catalyst, in addition to glucose, some traces of unreacted glycogen (60.6, 69.4, 71.2, 71.6, 71.8, 73.4, 76.8, 99.6 ppm) were also noticed (Fig. 6b), indicating that the hydrolysis is not complete. This fact can be explained because of the low content of the HSiW in the catalyst. According to the ICP analysis, the content of HSiW in the HSiW/G catalyst was found to be 2.5 wt%. In other words, the amount of HSiW in the 0.1 g HSiW/G catalyst used for the hydrolysis reaction is 0.0025 g. It is interesting to note that even at such a low loading of the solid acid, the synthesized catalyst is effective for the hydrolysis of glycogen. In addition, under the reaction conditions used, the hydrolysis of glycogen was selective. No by-products such as hydroxymethylfurfural (HMF), levulinic acid and formic acid were formed. When the hydrolysis of glycogen was previously performed with HCl in a microwave, these by-products were observed.[4]

For optimizing the glycogen hydrolysis process with HSiW/G and detailed study, the reaction was performed in a larger reaction batch of 20 mL at different reaction times, temperatures and wt/wt% ratio of catalyst and glycogen. The products obtained under various reaction conditions were analyzed by HPLC analysis, and the results are presented in Fig. 7.

A representative HPLC chromatogram recorded on the hydrolyzate obtained from the hydrolysis of glycogen is shown in Fig. S2.† The retention time was detected in control experiments with different amounts of glucose. The peak with a retention time of 12.3 min is attributed to glucose.

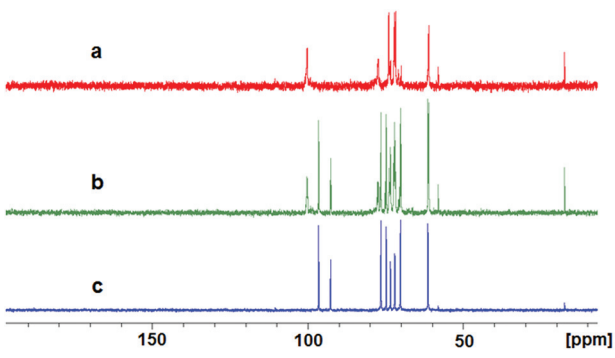

Fig. 6 ^{13}C NMR spectra of hydrolyzate obtained with (a) bare graphene, (b) HSiW/G and (c) HSiW (reaction conditions: 0.1 g glycogen; 0.1 g catalyst; 2 mL water; 100 °C; 1 h).

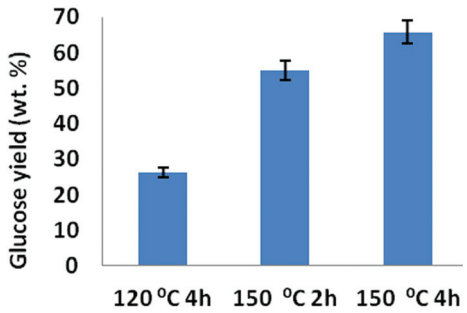

Fig. 7 Glucose yield (wt%) from glycogen hydrolysis as a function of reaction time and temperature (reaction conditions: 1 g glycogen; 1 g HSiW/G catalyst; 20 mL water).

After 2 h at 120 °C no glucose was found. The absence of glucose at 120 °C in the series of experiments with a large batch (20 mL) compared to the formation of glucose at 100 °C with the small batch (2 mL) is, probably, due to the higher volume needing a longer time and higher temperature to obtain the appropriate pressure in the vessel compared to the one used with the small batch. When the reaction time was increased at the same temperature, the yield of glucose was 26 wt% (Fig. 7).

At 150 °C after 2 h the yield of glucose was 55 wt%. Prolonging the reaction time to 4 h increased the glucose yield to 66 wt%. It is clear that higher temperatures lead to higher product yields. As a result, the reaction time of 4 h at 150 °C was chosen to be the optimal conditions with the highest yield of glucose.

The weight ratio of the catalyst (HSiW/G) to glycogen was varied in the range 1–0.25. The yields of glucose generated from hydrolysis of glycogen with various amounts of catalyst are depicted in Fig. 8.

It was observed that at a hydrolysis temperature of 150 °C for 4 h, the yield of glucose for all of the examined ratios of HSiW/G to glycogen (1 : 1; 0.5 : 1 and 0.25 : 1) was almost the same (65 wt%). When same amount of bare HSiW as that present in the supported catalyst (HSiW/G) was used as a cata-

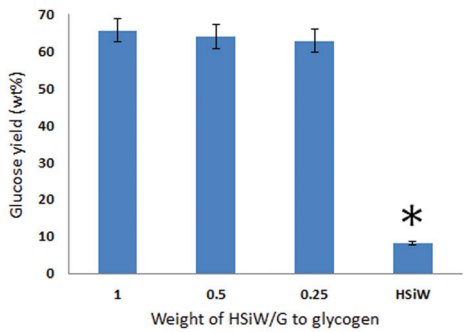

Fig. 8 Glucose yield from glycogen hydrolysis at different weight ratios of HSiW/G to glycogen (glycogen – 1 g; HSiW/G – 1, 0.5 and 0.25 g; time – 4 h; temperature – 150 °C). *Bare HSiW – 0.025 g (this corresponds to the amount of HSiW present in the HSiW/G catalyst at a ratio of HSiW/G to glycogen 1 : 1).

lyst, the glucose yield was dramatically low (8.2%). Thus, the bare HSiW is about 8 times less active than HSiW deposited on graphene. The increase of the catalytic activity of the supported HSiW compared to the bare HSiW could be due to the effective and uniform distribution of the heteropoly acid on the surface of graphene. Moreover, the HSiW/G catalyst has a larger specific surface area (52 $m^2 g^{-1}$) compared to bare HSiW (1.8 $m^2 g^{-1}$). The large surface area enables an effective contact between the uniformly distributed acid sites on the graphene surface and the glycogen that promotes the rapid, effective and efficient catalytic reaction.

The observed enhanced activity of HSiW/G could be due to the strong binding of the heteropoly anions to the aromatic π-cloud on the graphene surface (similar to π–π interactions) leading to higher accessibility of the protons for the cleavage of the glycosidic bond in glycogen. Kim *et al.* reported similar strong electrostatic interactions between polyoxometalate and rGO.[18] In contrast, in the case of bare HSiW, the protons of the polyanion rotate freely in the reaction medium and are in constant motion. As a result, the probable interaction between the protons and the reactant (glycogen) is low, resulting in lower yields of glucose.

We have further evaluated the stability of HSiW/G in the hydrolysis of glycogen. After the first run under optimal hydrothermal conditions (1 g HSiW/G, 1 g glycogen, 20 mL water, 150 °C, 4 h) the HSiW/G was separated from the aqueous product mixture by centrifugation. The collected catalyst was dried under vacuum overnight and subsequently reused for the second and third runs under identical reaction conditions. The results as measured by HPLC analysis are presented in Fig. 9.

The glucose yield after three reaction cycles was still high (63.3 wt%) indicating that HSiW can be reused without loss in catalytic activity. Even after three repeated runs, the amount of HSiW on graphene was found to be 2.2 wt%. This indicates that the catalyst is not just a physical mixture but a supported system wherein the active component (HSiW) is strongly adhered to the support (graphene). The good catalyst stability could be due to the use of the sonochemical deposition method which leads to the strong adherence of HSiW to the support.[40,41] The catalyst can serve also in a hydrothermal flow system, since the HSiW will not leach out easily.

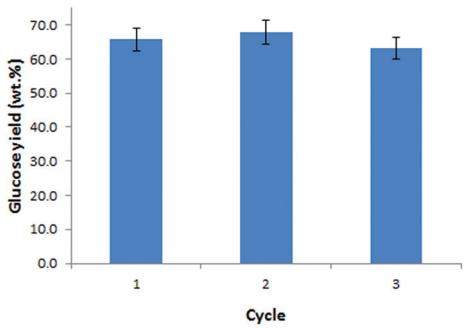

Fig. 9 Recyclability of the HSiW/G catalyst in the hydrolysis of glycogen (reaction conditions: 1 g of glycogen; 1 g of the solid acid catalyst; 20 mL of H_2O; 150 °C; 4 h). The catalyst was recovered by 9000 rpm centrifugation for reuse.

It is difficult to explain the excellent catalytic activity of HSiW/G in the hydrolysis of the glycosidic bond due only to the higher surface area and homogeneous deposition of HSiW on the graphene surface. Wei *et al.* attributed the excellent catalytic activity of sulfonated graphene oxide (sGO) in the hydrolysis of cellobiose and isoflavones to the interaction between the anions of the side chains of the catalyst and the reactants. In addition to hydrophilic groups, sGO has hydrophobic, flexible graphene sheets that can help to form hydrophobic cavities on the graphene surface. This adsorbent microregion has affinity for certain reactants.[21]

We suppose that the mechanism of interaction between HSiW/G and glycogen was similar to the one discussed in ref. 21. Namely, the hydrophobic graphene sheets of HSiW/G first provide hydrophobic cavities to the glycogen on the surface of the catalyst. Then the hydrophobic parts (carbon rings) of the glycogen are encapsulated by the graphene, and the hydrophilic parts (OH and O) form hydrogen bonds with the heteropoly acid on the graphene surface. In addition to the H^+ and different metal–oxygen bonds, the heteropoly acid inherently contains water molecules within the crystal structure that contribute to the hydrophilic nature of the catalyst. A combination of hydrophilic and hydrophobic regions on the catalyst surface leads to an increased concentration of glycogen on the catalyst surface and thereby contributes to the enhancement of hydrolysis rate and selectivity. Afterwards, the protons ionized from the catalyst support attack the glycosidic bond and catalyze the hydrolysis of glycogen. Finally, the glycosidic bond is broken owing to the hydrolysis of the reactant.

Therefore, the catalyst is prospective, selective, and efficient for biomass hydrolysis. Moreover, the usefulness of the catalyst was tested for the hydrolysis of cellulose under the optimal reaction conditions (4 h, 150 °C). A glucose yield value of 33 wt% was obtained, indicating the activity of the catalyst (HSiW/G) for cellulose hydrolysis. Therefore, the catalyst designed could be used for the hydrolysis of cellulosic biomass. Shimuzu *et al.* reported a glucose yield value of 15% in a $H_3PW_{12}O_{40}$ catalyzed cellulose hydrolysis process under hydrothermal conditions (150 °C, 2 h). Moreover, prior to the hydrolysis process, the cellulose was pretreated for 48 h under ball milling.[10] Tian *et al.* reported a glucose yield value of 50.5 wt% from the hydrolysis of cellulose in the presence of the $H_3P_{12}O_{40}$ catalyst under hydrothermal conditions (180 °C; 3 h).[11] A high glucose yield value of 75.6 wt% was reported by Li *et al.* from the hydrolysis of cellulose under microwave irradiation using conc. $H_3PW_{12}O_{40}$ as the catalyst.[42] The above comparison with the recent reports on cellulose hydrolysis clearly indicates the advantage of the current process being based on the use of a heterogeneous catalyst unlike the homogeneous nature of the catalyst reported.[10,11,42] Even under modest hydrolysis conditions glucose yield values of 33 and 66 wt% were obtained from cellulose and glycogen, respectively, using the HSiW/G catalyst.

For comparing the effect of the catalyst preparation method on its activity, glycogen hydrolysis was also carried out under identical reaction conditions, using the HSiW/G catalyst prepared by the impregnation method. A glucose yield value of 40 wt% was observed relative to the value of 66 wt% that was obtained using the catalyst prepared by the sonochemical route. In addition, the hydrolyzate was found to be acidic (pH 1–2) in the case of impregnation based catalysts unlike the near neutral (pH 6) nature of the hydrolyzate generated using sonochemical based catalysts. This result indicates a strong interaction between the HSiW and graphene in the catalyst prepared by the sonochemical method.

Experimental

Materials

Tungstosilicic acid hydrate ($H_4SiW_{12}O_{40}{\cdot}nH_2O$, HSiW, 99%), cellulose powder (Avicel® PH-101; ~50 μm particle size) and glycogen from bovine liver were purchased from Sigma-Aldrich Co. (St Louis, MO, USA). The graphene nanoplatelets (6–8 nm thick ×15 microns wide) were purchased from STREM chemicals, Newburyport, MA, USA. The chemicals were used without further purification.

Catalyst preparation

An ultrasound-assisted method was used to prepare the supported HSiW/G catalysts. Typically, the following procedure was followed: 2 g HSiW was first dissolved in 80 mL ethanol, followed by the addition of 2 g graphene. Owing to easy evaporation, ethanol is used as the solvent. The synthesis was performed in a glass beaker reactor of 120 mL volume. The mixture was sonochemically irradiated with 1 cm^2 titanium horn immersed 1 cm into the solution for 1 h with an efficiency of 40% (amplitude) with no external cooling (Sonicator 20 kHz, Sonics & Materials, VCX-750). After 1 h the temperature of the reaction slurry was 60 °C. The product was then collected by centrifugation and dried in a vacuum overnight.

In addition to the sonochemical route, the conventional impregnation method was also used for the preparation of the HSiW/G catalyst. The catalyst preparation process in the conventional impregnation method comprises of dissolving 2 g HSiW in 80 mL ethanol, followed by the addition of 2 g graphene. The mixture was kept for 4 h of stirring. Then the solvent was evaporated using a water bath followed by drying of the catalyst under vacuum overnight. The catalysts prepared in the two aforementioned routes were compared in the glycogen hydrolysis reaction.

Catalyst characterization

The XRD analysis of the HSiW/G was performed on a Bruker D8 diffractometer with Cu Kα – 1.541 Å radiation. The morphology and texture of the HSiW on the graphene were studied by transmission electron microscopy (TEM) JEOL JEM-1400 (120 kV) and high resolution scanning electron microscopy (HR-SEM), FEI Company TM MAGELLAN 500L (Holland). The particle size distribution of HSiW (dispersed in ethanol) was estimated by the DLS method using a Malvern Zetasizer Nano-series device (Malvern Instruments, Malvern, UK). The amount of HSiW deposited on graphene by sonication was determined by the inductively coupled plasma (ICP) method on the ULTIMA JY 2501 instrument. Surface area, pore volume and pore size distribution were measured using a Nova 3200e Quantachrome analyzer. The surface area was calculated from the linear part of the BET plot. The pore size distribution was estimated using the Barrett–Joyner–Halenda (BJH) model with the Halsey equation, and the pore volume was measured at the P/P_0 0.9947 signal point.

Fourier transform infrared (FT-IR) spectra were recorded using a FT-IR spectrometer (Bruker Tensor 27). Raman spectra were recorded using a Renishaw InVia Raman microscope equipped with a Leica DM2500 M analysis microscope (Leica Microsystems), sample focusing was done by a 50× (N.A. 0.75) lens. All the samples were irradiated by a 514 nm excitation wavelength with a constant power of ~0.25 mW.

Glycogen hydrolysis reaction

For the glycogen hydrolysis process a stainless steel homemade autoclave of 50 mL volume was used. Typically, 1 g glycogen and 1 g catalyst were dispersed in 20 mL water and placed in the autoclave. The autoclave was then placed in a regular air oven for the hydrothermal treatment of glycogen. Reaction parameters such as time, temperature of heating, weight ratio of the catalyst and glycogen were varied to optimize the hydrolysis process. In addition to glycogen, cellulose was also tested as carbohydrate feedstock for glucose production.

The reusability of the catalyst was investigated. After the reaction, the catalyst was separated from the solution by centrifugation and dried under vacuum overnight. The catalyst was used for a second run without regeneration under identical hydrothermal reaction conditions. The process was repeated 3 times.

The progress of the glycogen hydrolysis reaction was monitored using ^{13}C NMR spectroscopic analysis on a Bruker Avance DPX 300 instrument. D_2O was used as the solvent.

The water soluble products of catalyzed hydrolysis reactions were analyzed by HPLC (Merck-Hitachi LaChrom System L-7000 equipped with L-7455 Diode Array Detector and Schambeck SFD RI 2000 Refractive Index Detector, Bad Honnef, Germany). Analyses were carried out using a 300 × 7.8 mm Rezex-ROA ion exclusion chromatography column (Torrance, CA, USA) equipped with a matching guard column. The mobile phase used was 0.005 N H_2SO_4 under isocratic elution for 45 min at a flow rate of 0.5 mL min^{-1} at ambient temperature, with an injection volume of 10 μL. EZ Chrom Elite v. 3.1.7 software was used for data acquisition and processing, with the RI signal acquired using an external analog input. The content of the glucose in the hydrolyzate was calculated using a calibration curve obtained from a series of external glucose standards.

Conclusions

Polyoxometalate (HSiW) was deposited on the surface of graphene by the sonochemical method. Physico-chemical characterization of the HSiW/G catalyst was done using HR-SEM, TEM and XRD, which demonstrated a homogeneous distribution of HSiW on the surface of graphene supports. The catalytic performance of the synthesized catalyst was evaluated for the hydrolysis of the glycosidic bond of biomass to glucose. The following conclusions have been drawn: the catalytic activity of HSiW/G is significantly higher than that of the bare HSiW. The hydrolysis process with HSiW/G is selective, fast and green with a high yield of glucose (66 wt%). The sonochemical method provided strong anchoring of HSiW to graphene and high stability of the catalyst. The reuse of the HSiW/G catalyst in 3 cycles was demonstrated. The glucose yield after three reaction cycles was not altered significantly, showing that HSiW/G is a reusable, economically viable and green catalyst.

Acknowledgements

We thank the Israel Science Foundation for supporting this research by grant 12/586, and the Ministry of Science and Technology for the research grant 3-9802.

Notes and references

1 Y. B. Huang and Y. Fu, *Green Chem.*, 2013, **15**, 1095.
2 J. P. Lange, E. Heide, J. Buijtenen and R. Price, *ChemSusChem*, 2012, **5**, 150.
3 J. R. Regalbuto, *Science*, 2009, **325**, 822.
4 M. Klein, I. N. Pulidindi, N. Perkas, E. Meltzer-Mats, A. Gruzman and A. Gedanken, *RSC Adv.*, 2012, **2**, 7262.
5 G. Brodeur, E. Yau, K. Badal, J. Collier, K. B. Ramachandran and S. Ramakrishnan, *Enzyme Res.*, 2011, **2011**, 1.
6 I. N. Pulidindi, B. B. Kimchi and A. Gedanken, *Renewable Energy*, 2014, **71**, 77.
7 J. Tian, J. H. Wang, S. Zhao, C. Y. Jiang, X. Zhang and X. H. Wang, *Cellulose*, 2010, **17**, 587.
8 I. V. Kozhevnikov, *J. Mol. Catal. A: Chem.*, 2009, **305**, 104.
9 J. Macht, M. J. Janik, M. Neurock and E. Iglesia, *Angew. Chem., Int. Ed.*, 2007, **46**, 7864.
10 K. Shimizu, H. Furukawa, N. Kobayashi, Y. Itaya and A. Satsuma, *Green Chem.*, 2009, **11**, 1627.
11 J. Tian, J. Wang, S. Zhao, C. Jiang, X. Zhang and X. Wang, *Cellulose*, 2010, **17**, 587.
12 Y. Ogasawara, S. Itagaki, K. Yamaguchi and N. Mizuno, *ChemSusChem*, 2011, **4**, 519.
13 Z. Wang, F. Li, J. Xia, L. Xia, F. Zhang, S. Bi, G. Shi, Y. Xia, J. Liu, Y. Li and L. Xiam, *Biosens. Bioelectron.*, 2014, **61**, 391.
14 P. J. Wessely and U. Schwalke, *Appl. Surf. Sci.*, 2014, **29**, 83.
15 L. Kavan, J. Yum and M. Graetzel, *Phys. Status Solidi B*, 2013, **250**, 2643.
16 J. M. Yang, S. A. Wang, C. L. Sun and M. D. Ger, *J. Power Sources*, 2014, **254**, 298.
17 S. M. Choi, M. H. Seo, H. J. Kim and W. B. Kim, *Carbon*, 2011, **49**, 904.
18 Y. Kim and S. Shanmugam, *ACS Appl. Mater. Interfaces*, 2013, **5**, 12197.
19 Z. Cui, C. X. Guo, W. Yuan and C. M. Li, *Phys. Chem. Chem. Phys.*, 2012, **14**, 12823.
20 D. Verma, R. Tiwari and A. K. Sinha, *RSC Adv.*, 2013, **3**, 13265.
21 Z. Wei, Y. Yang, Y. Hou, Y. Liu, X. He and S. Deng, *ChemCatChem*, 2014, **6**, 2354.
22 M. Kitano, D. Yamaguchi, S. Suganuma, K. Nakajima, H. Kato, S. Hayashi and M. Hara, *Langmuir*, 2009, **25**, 5068.
23 S. Aikawa, Y. Izumi, F. Matsuda, T. Hasunuma, J. S. Chang and A. Kondo, *Bioresour. Technol.*, 2012, **108**, 211.
24 S. Aikawa, A. Joseph, R. Yamada, Y. Izumi, T. Yamagishi, F. Matsuda, H. Kawai, J.-S. Chang, T. Hasunumabch and A. Kondo, *Energy Environ. Sci.*, 2013, **6**, 1844.
25 N. Perkas, P. Gunawan, G. Amirian, Z. Wang, Z. Zhong and A. Gedanken, *Phys. Chem. Chem. Phys.*, 2014, **16**, 7521.
26 N. Perkas, J. Teo, S. Shen, Z. Wang, J. Highfield, Z. Zhong and A. Gedanken, *Phys. Chem. Chem. Phys.*, 2011, **13**, 15690.
27 V. Jafari, A. Allahverdi and M. Vafaei, *Adv. Powder Technol.*, 2014, **25**, 1571.
28 H. Atia, U. Armbrusterb and A. Martin, *J. Catal.*, 2008, **258**, 71.
29 P. S. Wate, S. S. Banerjee, A. Jalota-Badhwar, R. R. Mascarenhas, K. R. Zope, J. Khandare and R. D. K. Misra, *Nanotechnology*, 2012, **23**, 415101.
30 J. Chen, X. Fang, X. Duan, L. Ye, H. Lin and Y. Yuan, *Green Chem.*, 2014, **16**, 294.
31 J. Hodkiewicz, Thermo Fisher Scientific Inc. Application Note, 51946, 2010, 1.
32 L. M. Malard, M. A. Pimenta, G. Dresselhaus and M. S. Dresselhaus, *Phys. Rep.*, 2009, **473**, 51.
33 S. Zhu, Y. Zhu, X. Gao, T. Moa, Y. Zhu and Y. Li, *Bioresour. Technol.*, 2013, **130**, 45.
34 N. Legagneux, J. M. Basset, A. Thomas, F. Lefebvre, A. Goguet, J. Sa and C. Hardacre, *Dalton Trans.*, 2009, 2235.
35 A. Gedanken, *Ultrason. Sonochem.*, 2004, **11**, 47.
36 A. Gedanken, *Ultrason. Sonochem.*, 2007, **14**, 418.
37 J. Luo, Z. Fang and R. L. Smith Jr., *Prog. Energy Combust. Sci.*, 2014, **41**, 56.
38 S. D. Shewale and A. B. Pandit, *Carbohydr. Res.*, 2009, **344**, 52.
39 I. N. Pulidindi and A. Gedanken, in *Springer Book Series Production of Biofuels and Chemicals: Ultrasound*, ed. Z. Fang, L. s. Fan, J. R. Grace, Y. Ni, N. R. Scott and R. L. Smith Jr., 2015, ch. 6, p. 159.
40 V. G. Pol, D. N. Srivastava, O. Palchik, V. Palchik, M. A. Slifkin, A. M. Weiss and A. Gedanken, *Langmuir*, 2002, **18**, 3352.
41 I. Perelshtein, E. Ruderman, N. Perkas, T. Tzanov, J. Beddow, E. Joyce, T. J. Mason, M. Blanes, K. Moll, A. Patlolla, A. I. Frenkel and A. Gedanken, *J. Mater. Chem. B*, 2013, **1**, 1968.
42 X. Li, Y. Jiang, L. Wang, L. Meng, W. Wang and X. Mu, *RSC Adv.*, 2012, **2**, 6921.